

## Empirical and Numerical Study of Gas Turbine Disks under Mechanical Stress and Temperature Gradient

Rasoul Yari<sup>1,2</sup>, Hamid Zarepour<sup>1,2\*</sup>, Aazam Ghassemi<sup>1,2</sup>

<sup>1</sup>Department of Mechanical Engineering, Najafabad Branch, Islamic Azad University, Najafabad, Iran

<sup>2</sup>Modern Manufacturing Technologies Research Center (MMTRC), Najafabad Branch, Islamic Azad University, Najafabad, Iran

\*Email of Corresponding Author: h-zare@iaun.ac.ir

Received: October 12, 2019; Accepted: January 3, 2020

### Abstract

Gas turbine disks usually operate at very high temperatures and rotate at very high angular velocities under normal working conditions. High temperature in turbine disks causes changes in their properties. High angular velocity creates a large centrifugal force in the disk and high temperature reduces the strength of the material and causes deformation. Complexity of these parameters has turned the determination of stress distribution in gas turbine disks to one of the bottlenecks in the analysis, design and manufacturing of turbine engines. Therefore, using an applicable method for stress analysis is essential in order to better determine stress distribution in turbine disks. In this study, the finite element method (FEA) is used for predicting the behavior of rotating disks under mechanical and thermal stresses. In order to increase the certainty of simulation, gas turbine disk is first simulated and analyzed based on dimensions and loading conditions extracted from previous studies. Then, the results are compared with previous studies in order to determine the accuracy of analysis method applied in ANAQUUS software. Afterwards, gas turbine disks are evaluated under both rotational movement and temperature gradient. The results show that the presence of angular velocity and centrifugal force cause expansion to the disk radius. Finally, the conditions of the disk under the same rotational speed and temperature gradient applied for experiments are simulated and modeled in ABAQUS. The results show an acceptable correlation between the results of empirical and numerical studies. High angular velocity causes high centrifugal force in the component and increases stress especially at weak points. An increase in temperature also reduces the strength of the disk material and increases its deformation. According to the results, the approach proposed in this study is a suitable method for analysis of the stress, temperature and displacement in turbine disks and other components with similar functions.

**Keywords:** Gas Turbine Disks, Mechanical Stress, Temperature Gradient, Finite Element Analysis (FEM)

### 1. Introduction

Gas turbines are widely used in electric power generation and gas-line compressors as well as in cargo ships, trains, automobiles and turbojets engines. Gas turbine disks usually work under very high temperatures and angular velocities. The amount and distribution of the stress in rotating disks are the main limiting factors in their design [1]. In rotating disks, it is recommended to employ disks with variable thickness as the disks with constant thickness are uneconomical to use [2]. Eraslan [3] proposed a theoretical solution for the analysis of rotating disks with variable

exponential thickness. Eraslan et al. [4] also calculated the limit of angular velocity for rotating disks with variable exponential thickness.

Seireg and Surana [5] analyzed symmetrical disks under angular velocity without temperature gradient. In order to calculate peripheral and radial stresses inside a heterogeneous rotating disk with high rotational velocity, they divided the disk into several segments with constant thickness and used equilibrium equations to calculate stress for each segment. They ignored the effects of temperature gradient in their analysis. Ray and Sinha [6] first divided a rotating disk with variable thickness into several rings and then analyzed the rings separately. Chern and Prager [7] proposed similar analyses for rotating disks. Fox [8] used feasible direction method based on thermal gradient calculation to analyze the gas turbine disks. Cheu [9] used two methods of feasible direction and sequential linear programming to determine the geometry of gas turbine disks. His main goal was to reduce the disk weight under geometrical and stress limitations. Luchi et al. [10] determined the thickness in several locations on the disk and extracted general profile graphs by connecting these points to each other. They used triangular mesh to calculate the values of stress and displacement inside the disk at each step. Farshi et al. [11] calculated the stress in a heterogeneous disk under temperature gradient by dividing the disk into several rings. Jahed et al. [12] used the method of dividing the disk into several rings to propose a semi-analytical method for weight optimization in heterogeneous rotating disks under temperature gradients. Brujic et al. [13] used CATIA software to create parametric models for a gas turbine disk. Derakhshan et al. [14] designed the axial turbine of a small hydro-power plant. They used CATIA software to simulate the turbine and the results of their simulation showed a limited efficiency for axial turbine. The common method for mechanical attachment of fins into disk is via dove-tail slots on disk rim which limit the disk speed due to stress concentration in slots location. Another limitation of this method is that clamps on the disk rim which act against fin forces, add dead weight to the disk. One solution to overcome above problems is to create a rotor disk with integrated blades known as blisk [15, 16]. Non-integrated rotor disk design increases the engine size and complexity, giving rise to a lower engine durability and higher production cost [17].

Better performance and reliability as well as lower imbalance are among the advantages of the blisk turbines with blades made from the same material as the disk and its other components. Blisk turbines significantly reduce complexity and weight of the engines and their durable structure means better performance with lower hardware costs. The main challenges in manufacturing of the blisk turbines are high cost and complexity of the machining process [18, 19]. Since new engine blades are three dimensional and blisk manufacturing process for them is difficult and time-consuming, it is necessary to introduce more cost-effective methods for their manufacturing. Recent technological advances have made possible to use processes such as linear frictional welding to replace damaged blades in blisk structures. Based on the engine performance and geometrical characteristics, engine type and tolerances, various methods are used to attach the turbine to the engine shaft and transferring turbine torque to shaft and compressor. These methods include integrated rotors, splines, press fitting, welding, torque ring in self-containing disk, and hybrid methods. Disks can also be attached to shafts using simultaneous shrink and press fitting in order to ensure coaxiality between the disk and shaft as well as to increase their strength for proper transfer of torque to the shaft [20]. Rosyid et al. [21] only attempted the finite element analysis of

heterogeneous disks under mechanical and thermal stresses and investigated a disk at temperature of 800 °C and rotational speed of 15000 rpm. They used axial symmetry method for their analysis and reported that the maximum displacement takes place at the outer diameter of the disk while the maximum stress is observed in the thin part of the disk. Zharfi et al. [22] investigated the effect of temperature and particle distribution on creep behavior of rotating disks made of functionally graded materials (FGMs). They analyzed the disk at temperature of 300 °C and like previous studies only used software analysis.

In the previous studies, most of the researchers have attempted numerical analysis of the rotating disks and have rarely performed empirical studies. Most of the studies about rotating disks also ignore the changes in materials properties with changes in temperature. Therefore, the present study aims to analyze a rotating disk with properties dependent on the temperature. A finite element simulation of the heterogeneous gas turbine disks under mechanical stress, thermal gradient, and rotational movement is first presented by using temperature – displacement model and axial symmetry. Then, a sample of the disk is fabricated and studied under experimental conditions with a temperature of 800°C and rotational speed of 1000rpm. Subsequently, the experimental results are compared with the results of the software analysis.

## 2. Validation of the FEA results from ABAQUS

In order to validate the simulation process performed in ABAQUS, first a gas turbine disk with dimensions and loading conditions presented in references [9, 12] is simulated and analyzed. Then, the results are compared to those reported in [9, 12] to determine the validity of the software analysis results.

### 2.1 Simulation of the rotating disk

In order for modeling to be close to real conditions, four different types of loading were applied:

1. *Rotational force*: with the assumption of rotational speed equal to 22000rpm [9, 12]
2. *Loading force caused by blades*: a uniformly distributed load of  $P=165\text{MPa}$  which affects the outside layer of the disk radially [9, 12]
3. *Load caused by assembly pressure*: a uniformly distributed pressure caused by assembly of disk and shaft  $q=40\text{MPa}$ , affecting the inner part of the disk radially [24]
4. *Thermal loading*: temperatures at inner and outer diameters of the modeled disk are assumed to be  $T_i=28^\circ\text{C}$  and  $T_o=252^\circ\text{C}$ , respectively [9, 12].

In the research works reported in [9, 12], a steel disk with inner radius of 20.32mm and outer radius of 123.2mm rotating at speed of 22000rpm was optimized. Linear programming method and acceptable direction algorithm were employed for the disk optimization in [9]. While in [12], the disk was optimized by dividing it into rings.

### 2.2 Comparison between the results of numerical analysis in this research and other studies

Figure 1 presents the diagram for the disk profile thickness versus disk radius reported in [9, 12] along with the results of the present study. Figure 2 also shows the comparison between the results of stress distribution reported in [9, 12] and those of the present study. The similarity of these

graphs shows that the results of stress analysis in this study have a good correlation with the results reported in [9, 12].

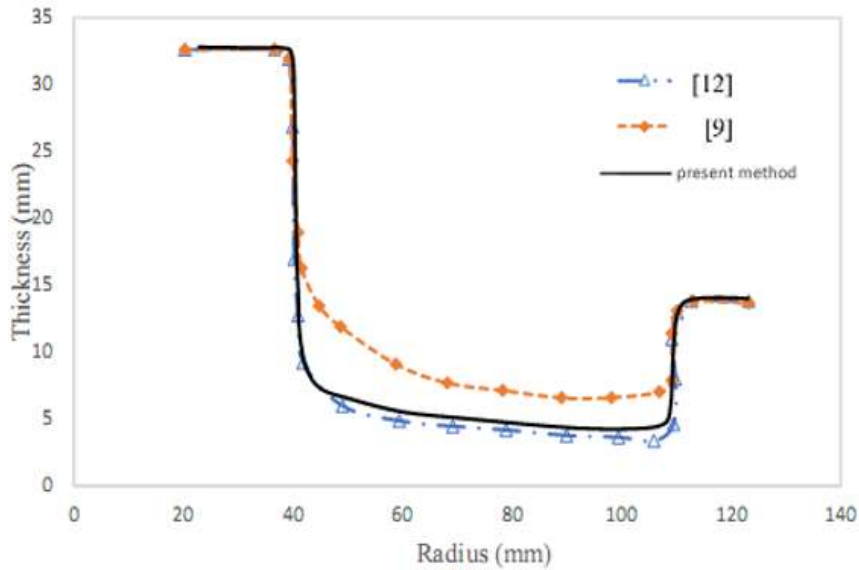


Figure1. Results of the disk profile thickness versus disk radius in [9, 12] and present study

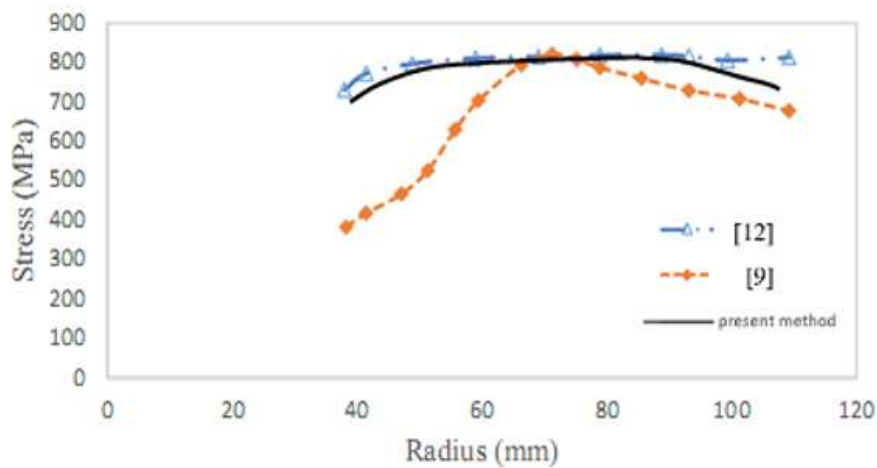


Figure2. Results of the disk stress distribution in [9, 12] and present study

### 3. Experimentation

A sample disk with CK45 carbon-steel material was made on a TN50D lathe machine. The disk dimensions are shown in Figure 3. The properties of the CK45 steel are shown in Tables 1 and 2(a, b) [23]. Table 3 shows the properties of this material with yield strength of 420MPa at various temperatures [24]. As depicted in Figure 4, the disk was assembled on a mandrel and fixed into machine chuck with providing enough space for heating and temperature measurement of the disk. In the next step, the disk was rotated at speed of 1000 rpm and heated with a gas torch at a suitable distance in order for the flame to only reach the periphery of the disk. During heating, it is necessary to keep the flame stable and at a constant distance of 50 mm from the disk for the entire experiment to produce a uniform temperature on the disk (Figure 5). The temperature of the disk surface is constantly measured using a laser thermometer model FLUKE 568 (Figure 6). Then, the

heating time is recorded for various disk temperatures at 250, 500, 600 and 800°C. The results of the experimental tests at different parameter settings are presented in Table 4. In all experiments, the rotational speed of the disk was kept constant at 1000 rpm. In order for the disk to reach the necessary temperature for each experiment, the heating was carried out for a certain time duration which is determined based on the preliminary tests. As can be seen in table 4, an increase in temperature causes the expansion in the part while angular velocity and centrifugal force increase the diameter of the disk. Figure 7 shows the increase in the outer diameter of the disk with rising the temperature.

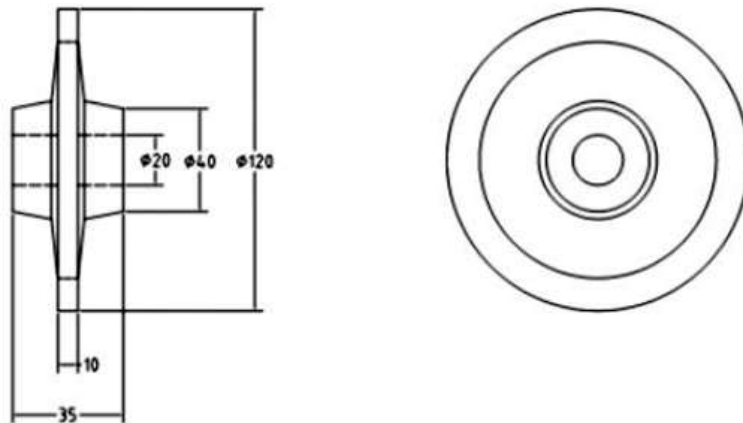


Figure3. The geometrical shape of investigated disk

Table1. Properties of the CK45 carbon-steel [23]

| Yield strength           | Tensile strength         | Thermal expansion                            | Thermal conductivity      | Specific heat                                  | Density               | Poisson's ratio | Young's modulus |
|--------------------------|--------------------------|--|---------------------------|--|-----------------------|-----------------|-----------------|
| 420<br>N/mm <sup>2</sup> | 750<br>N/mm <sup>2</sup> | 1.17<br>$\times 10^{-5} \frac{1}{^{\circ}K}$ | 15 $\frac{W}{m^{\circ}K}$ | 0.45<br>$\times 10^{-3} \frac{J}{Kg^{\circ}K}$ | 7800 $\frac{Kg}{m^3}$ | 0.3             | 210GPa          |

Table2 (a). CK45 carbon-steel chemical composition

| C         | Mn        | Si   | Cr   | Ni   | Mo   | P     | S         |
|-----------|-----------|------|------|------|------|-------|-----------|
| 0.42-0.50 | 0.50-0.80 | 0.40 | 0.40 | 0.40 | 0.10 | 0.035 | 0.02-0.04 |

Table 2 (b). Hot work and heat treatment temperatures

| Forging     | Normalization | Subcritical annealing | Isothermal annealing | Hardening  | Tempering        |            |
|-------------|---------------|-----------------------|----------------------|------------|------------------|------------|
| 1100~850 °C | 840~880 °C    | 650~700 °C            | 820~860 °C           | 600 °C x1h | 820~860 °C water | 550~660 °C |

Table3. Properties of the disk material with yield strength of 420MPa at high temperatures [25]

| Young's modulus (Gpa) | Temperature (°C) |
|-----------------------|------------------|
| 14                    | 900              |
| 27                    | 700              |
| 147                   | 400              |
| 189                   | 200              |
| 210                   | 100              |
| 210                   | 20               |



Figure4. The placement of disk on the shaft and their location on drilling chuck

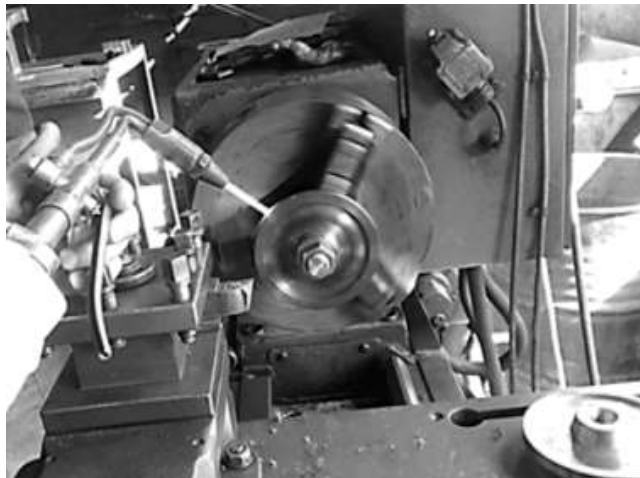


Figure5. Heating method of the disk



Figure6. FLUKE 568 thermo-Laser instrument and temperature control method

Table4. Results of the experimental tests at various parameter settings

| Test No. | Temp. (°C) | Time (s) | Outer dia. at 28 °C (mm) | Outer dia. at test temp. (mm) | Outer dia. increase (mm) | Radius increase (mm) |
|----------|------------|----------|--------------------------|-------------------------------|--------------------------|----------------------|
| 1        | 250        | 120      | 119.73                   | 120.05                        | 0.32                     | 0.16                 |
| 2        | 500        | 330      | 119.73                   | 120.47                        | 0.64                     | 0.32                 |
| 3        | 600        | 400      | 119.73                   | 120.53                        | 0.80                     | 0.40                 |
| 4        | 800        | 600      | 119.73                   | 120.79                        | 1.04                     | 0.52                 |

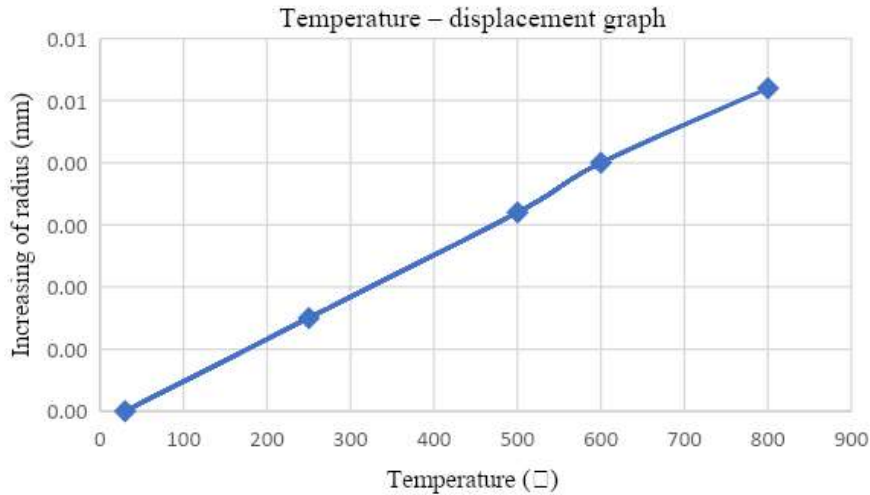


Figure7. Experimental results of the disk radius increase with temperature

#### 4. FEM simulation of the disk based on the experimental conditions

In this section, the disk used for empirical tests is simulated and analyzed in ABAQUS finite element analysis software. In order to define boundary conditions, the rotational speed is set to  $\omega=1000\text{rpm}$ , the initial disk temperature to  $T_i=25^\circ\text{C}$ , and the outer surface temperature of the disk to  $T_0=800^\circ\text{C}$ . The meshing was selected from type CAX6MT with the size of 0.001mm. The time necessary for the disk to reach the test temperature is shown in Table 4. In this study, various analyses were carried out to determine the proper heat flux, five of which are shown in Table 5. In order to determine the proper heat flux software, the heating time was considered constant and equal to 600 sec. Then, a rough heat flux number e.g.  $15000\text{ W/m}^2$  was entered and the simulation was started. The results were then extracted and the temperature of the disk surface was determined. In this study, a heat flux of  $15000\text{ W/m}^2$  yielded a disk surface temperature of  $120^\circ\text{C}$ . Then, the heat flux number was changed by trial and error, until surface temperature of the disk reached  $800^\circ\text{C}$ . Finally, a heat flux of  $115000\text{ W/m}^2$  yielded a disk surface temperature of  $820^\circ\text{C}$ .

Table5. Trial and error table for determining the heat flux

|   | Heat flux ( $\text{W/m}^2$ ) | Time duration (s) | Disk surface temp. ( $^\circ\text{C}$ ) |
|---|------------------------------|-------------------|---|
| 1 | 10000                        | 600               | 94                                      |
| 2 | 15000                        | 600               | 120                                     |
| 3 | 50000                        | 600               | 302                                     |
| 4 | 120000                       | 600               | 850                                     |
| 5 | 115000                       | 600               | 820                                     |

4.1 Numerical analysis with angular velocity parameter

In this section, the gas turbine disk was analyzed under four different angular velocities ( $\omega$ ) including 1000, 10000, 20000 and 40000 rpm. In this analysis, similar meshing was used in different loading conditions. In all rotational speeds, the geometrical dimensions of the disk were similar. Mechanical and thermal stresses were also constant, the value of which are presented in Table 6. In Figure 8, the locations defined on the disk surface for drawing the graph are shown. Figure 9 shows the distribution of Von Mises stress in the loading condition 3 with 20000 rpm rotational speed. As can be seen in Figure 9, the maximum stress is applied to the inner ring of the disk. Figure 10 shows the distribution of Von Mises stress in the *a-f* path (Figure 8).

In Figure 11, the displacement distribution graph under condition 4 and rotational speed of 40000 rpm is shown. The maximum displacement happens on the outmost part of the disk which is equal to 0.5mm at the rotational speed of 40000 rpm in the radial direction, while the minimum displacement (equal to 0.19mm in the radial direction) is seen at the innermost part of the disk. Due to symmetry of the disk, no significant deformation is seen in the disk and only precise measurements can determine the changes in disk dimensions.

Table6. Stress values in the turbine disk

|  |                   |
|--|-------------------|
| Stress in the inner part of the disk due to assembly | $q=40Mpa$         |
| Stress in the outer part of the disk due blades      | $p=200MPa$        |
| Initial disk temperature                             | $T_i=28^\circ C$  |
| Disk surface temperature                             | $T_0=252^\circ C$ |

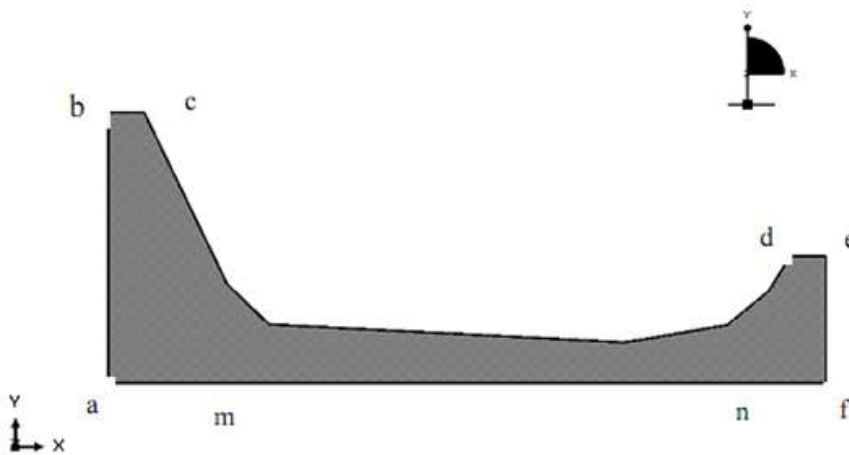


Figure8: Defined paths on the disk for displacement graphs



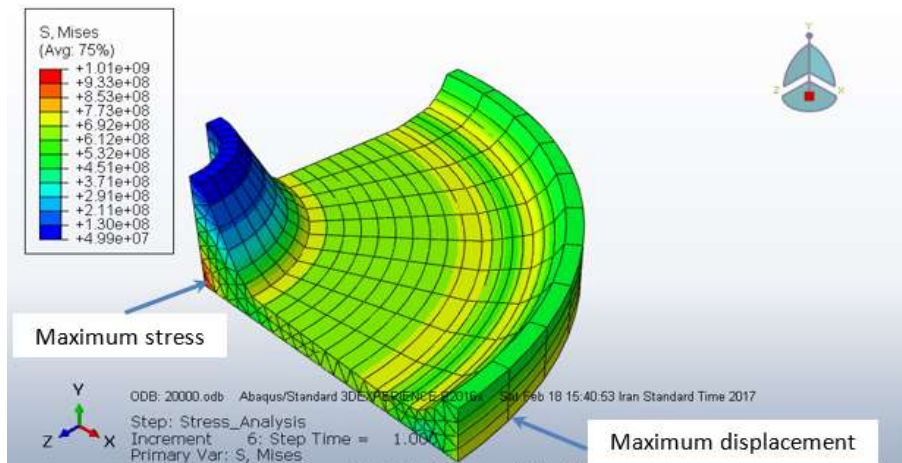


Figure9. Distribution of Von Mises stress in the loading condition 3 with 20000 rpm

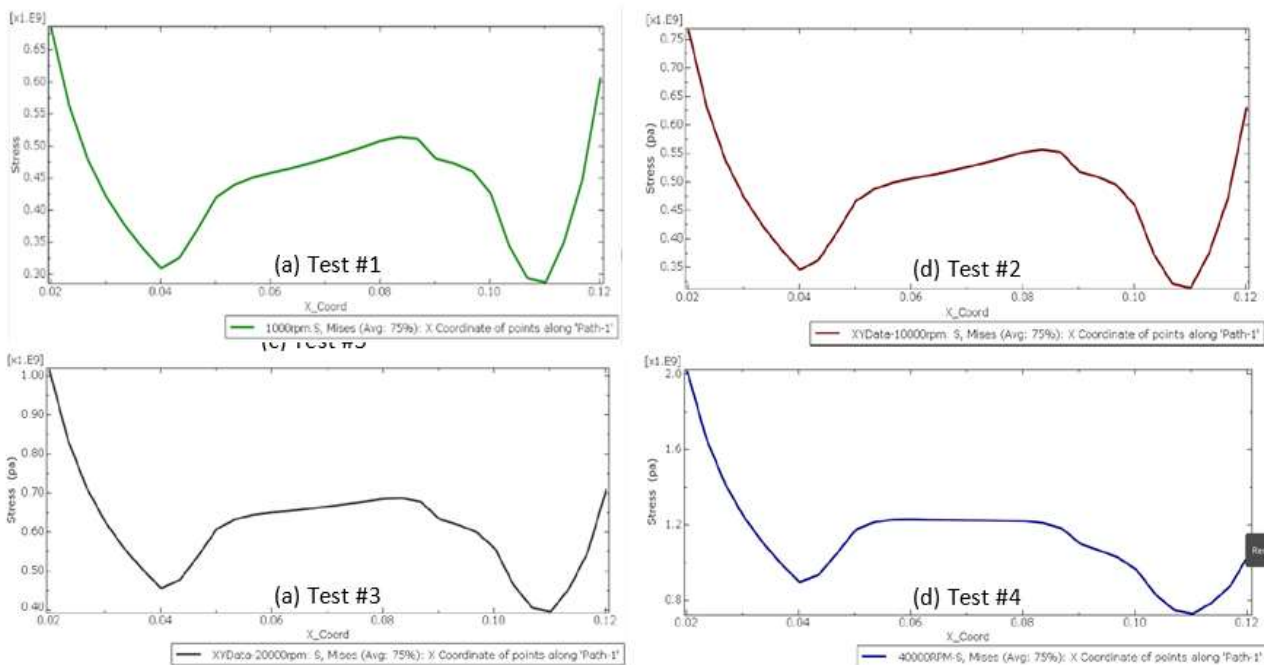


Figure10. Distribution of Von Mises stress in the *a-f* path

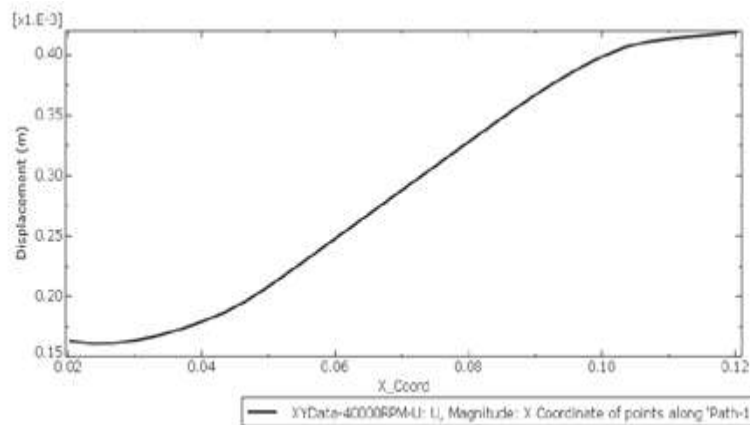


Figure 11. Displacement distribution at radius path in condition 4

#### 4.2 Results of the finite element analysis of the disk at different angular velocities

The stress distribution graphs at rotational speeds of 1000, 10000, 20000 and 40000 rpm are shown in Figure 10. With increasing the angular velocity, the stress on the disk increases. Due to the symmetry of the disk, the stress on the disk increases uniformly for all parts of the disk. As can be seen in these graphs, maximum stress is present in the inner ring of the disk which is due to high centrifugal force at that location as shown in Figure 9. Another part of the disk with high stress is the disk edge having the smallest thickness compared to other locations. The maximum displacement is also related to the outermost point of the disk (Figure 11) which is affected by centrifugal force and is directly dependent on it while the least displacement occurs in the inner diameter of the disk.

#### 4.3 Results of the disk FEA using experimental tests conditions

Four experimental tests are simulated and analyzed using ABAQUS. Figure 12 shows the temperature distribution in the experiments. The temperature distribution graph on the disk radial direction for the experiments is shown in Figure 13. Displacement distribution of the disk in four experiments is shown in Figure 14 while Figure 15 shows the displacement in the radius direction of the disk. Horizontal axis is the normalized disk radius path while the vertical axis is the displacement in meters. Figure 16 shows the distribution of Von Mises stress in the disk during tests while the distribution of Von Mises stress in the disk radial direction is shown in Figure 17. The results of the simulation which is based on the four empirical tests are shown in Table 7. As can be seen from the results, the stress is reduced with increasing the temperature. This is due to the fact that Young's modulus of the disk material decreases with temperature rising. In the analysis number 4, due to temperature increase to 800 °C, the Young's modulus significantly decreases as evidenced in Table 3 and therefore the resulting stress is very low. The results of displacement and temperature distributions on the disk show that the highest temperature and displacement values are at the outer edge of the disk which could be ascribed to the high temperature at the outer edge of the disk due to closeness to heat source as well as the high centrifugal force that creates displacement in the outer edge of the disk.

Table7. The results of limited element analysis

| Test No. | Time | Max temp. (outer edge) (°C) | Min temp. (inner edge) (°C) | Max disp. (outer edge) (mm) | Min disp. (mm) | Max. stress (MPa) |
|----------|------|-----------------------------|-----------------------------|-----------------------------|----------------|-------------------|
| 1        | 120  | 254                         | 95                          | 0.11                        | 0.012          | 156               |
| 2        | 330  | 507                         | 333                         | 0.28                        | 0.04           | 112               |
| 3        | 400  | 558                         | 414                         | 0.34                        | 0.04           | 80                |
| 4        | 600  | 821                         | 647                         | 0.49                        | 0.07           | 86                |

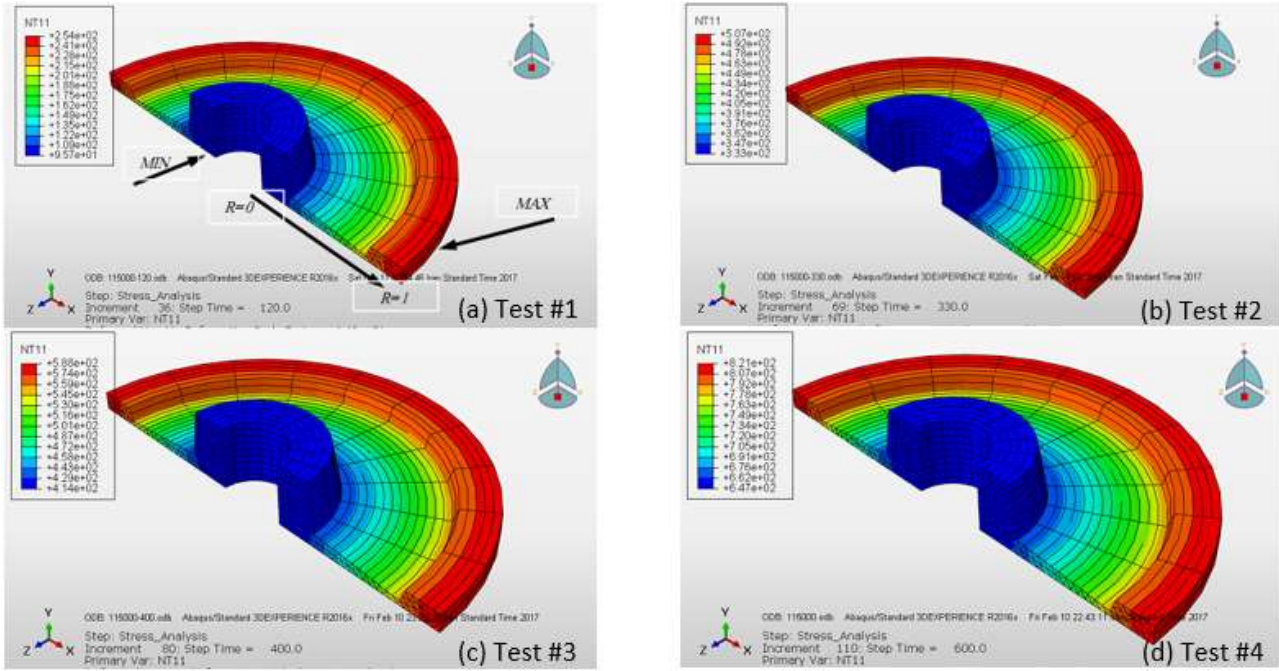


Figure12. Temperature distribution on the disk surface

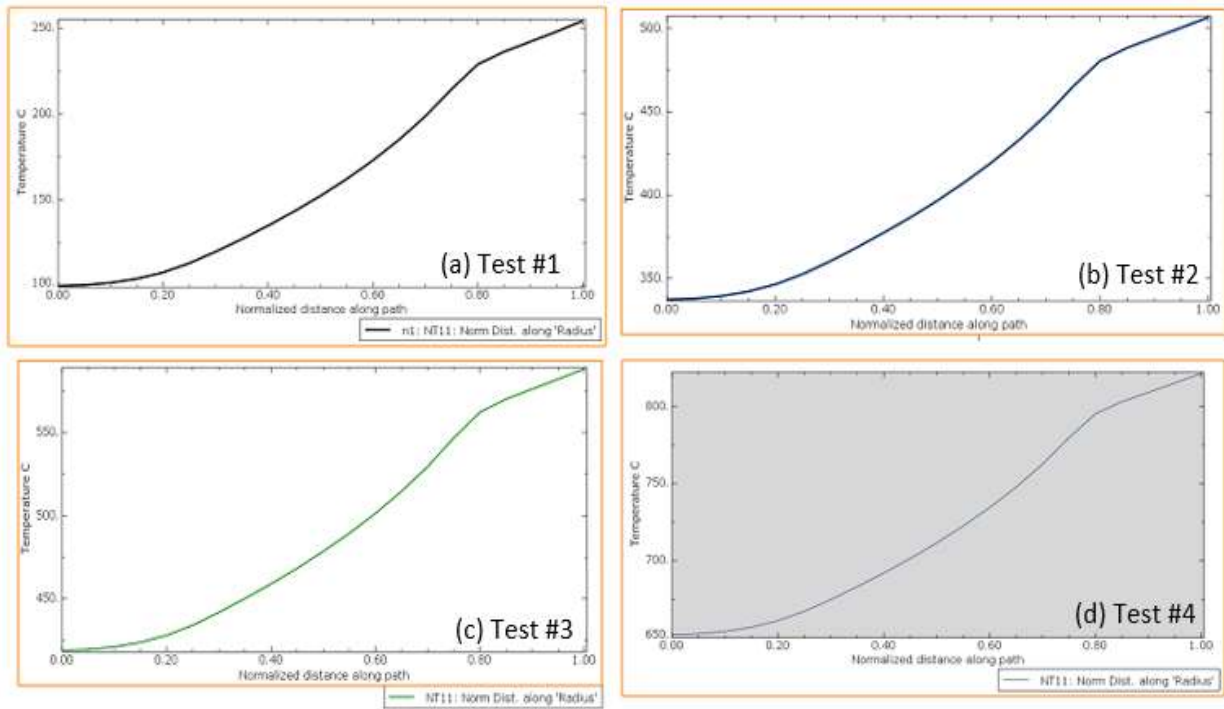


Figure13. Temperature distribution on the disk radius path

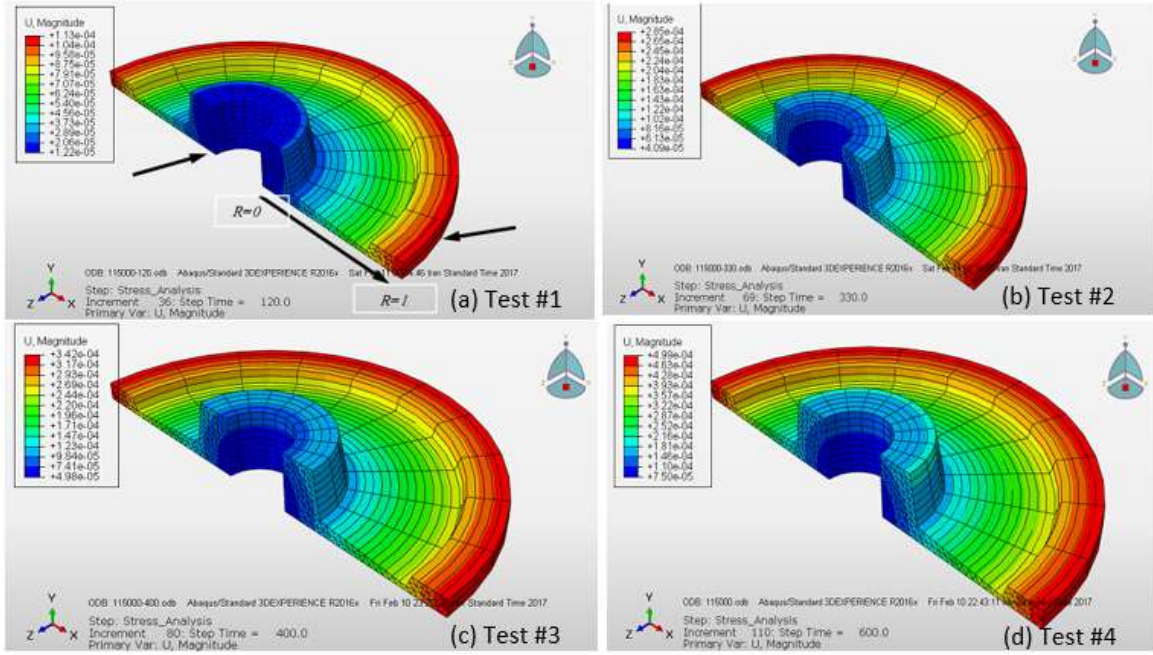


Figure14. Displacement distribution on the disk surface

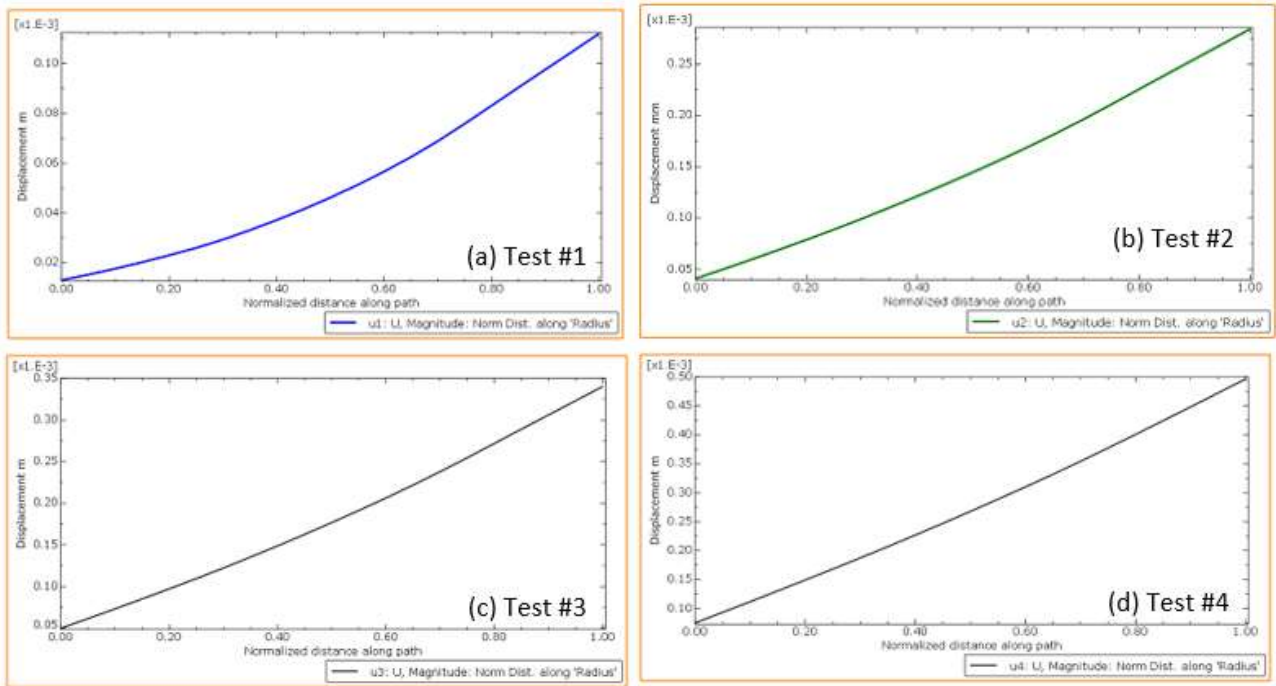


Figure15. Displacement distribution in the disk radial direction

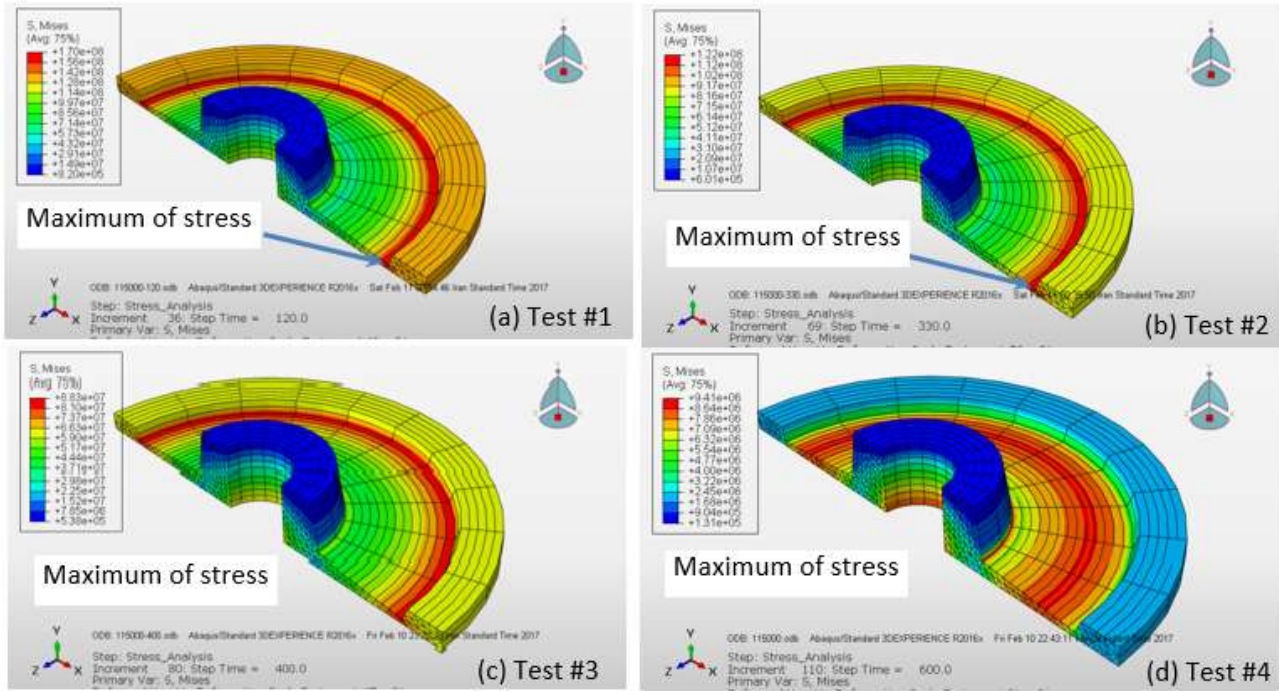


Figure16. Von Mises stress distribution in the disk

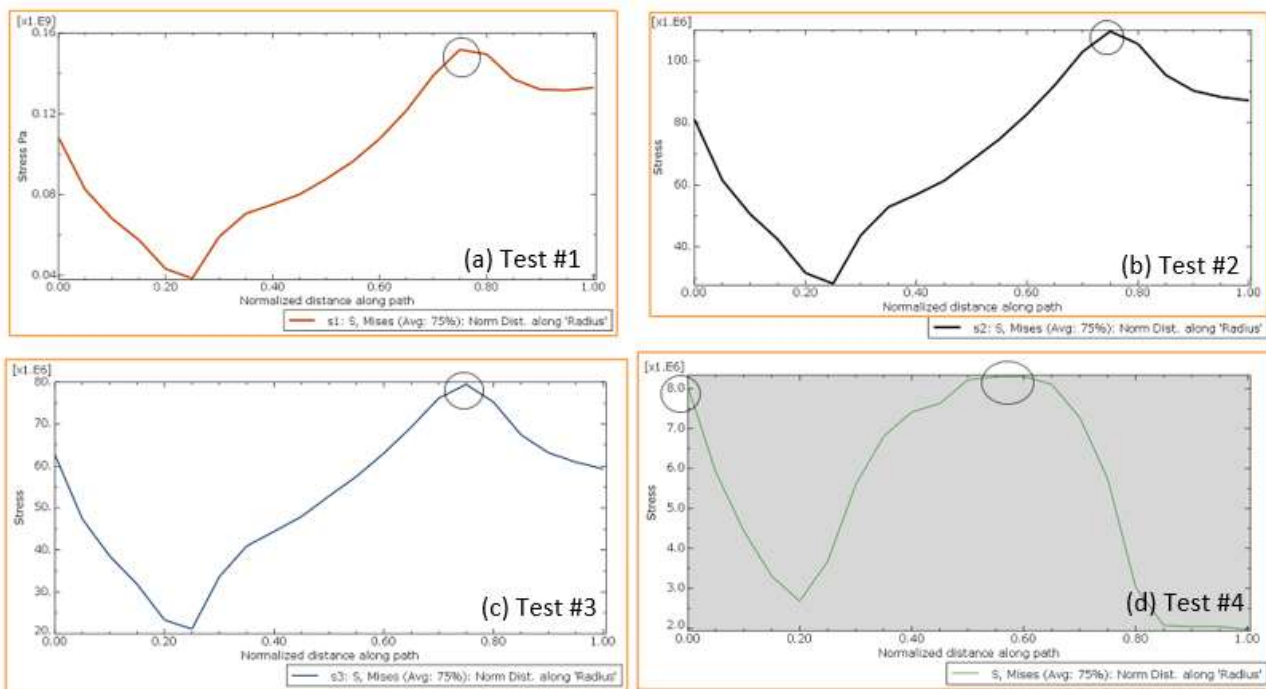


Figure17. Von Mises stress in the disk radial direction

#### 4.4 Comparison between empirical and numerical studies

An increase in temperature causes expansion in the disk while an increase in both centrifugal force and angular velocity results in an increased disk radius. The changes in the outer diameter of the disk versus temperature variations for empirical tests and finite element analysis at four temperature levels of 250, 500, 600 and 800 °C are shown In Figure 18. According to the graphs presented in

Figure 18, it can be concluded that there is a negligible difference between the results of the experimental tests and finite element analysis. Therefore, it can be said that there is a good correlation between empirical and numerical results.

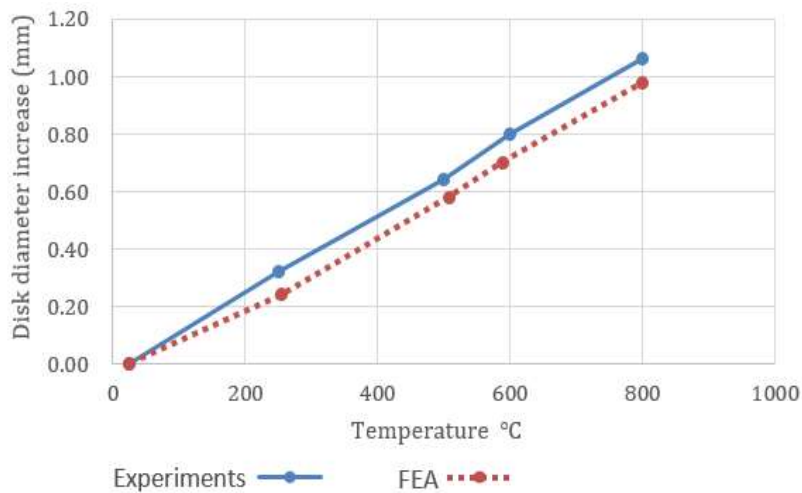


Figure18. Variations of the disk outer diameter vs. temperature for experiments and FEA

## 5. Conclusion

In this study, finite element analysis was employed for predicting the behavior of rotating disk under mechanical and thermal stresses. First, in order to ensure the validity of finite element analysis in ABAQUS software, gas turbine disk with dimensions and loading conditions extracted from previous works was simulated. The results were then compared to the results in previous works in order to evaluate the validity of ABAQUS finite element analysis results. In the next step, a gas turbine disk was investigated using empirical tests. The results showed that an increase in temperature causes expansion of the disk. Moreover, an increase in both angular velocity and centrifugal force leads to an increased disk diameter. In the final step, the rotating disk and temperature gradient used in empirical studies were modeled and analyzed in ABAQUS software. The results showed that there is a good correlation between numerical and empirical results which is evident in temperature – displacement graphs. Angular velocity causes high centrifugal force in the disk and increases stress especially in thin parts of the disk. Temperature increase also reduces the strength of the materials used in the disk and increases its deformation. Based on the results, the method used in this work is a suitable method for analyzing the stress, temperature and displacement distributions in turbine disks and similar parts in order to achieve better conditions for stress, temperature and displacement distributions.

## 6. References

- [1] Bar, W., Orkisz, M. and Moustapha, H. 2014. Multidisciplinary Design and Optimization of Gas Turbine Engine Low Pressure Turbine at Preliminary Design Stage. *Journal of KONES Powertrain and Transport*. 21(3): 15-22.
- [2] Liu, J. S., Parks, G. T. and Clarkson, P. J. 2002. Optimization of Turbine Disk Profiles by Metamorphic Development. *Journal of Mechanical Design*. 124(2): 192-200.

- [3] Eraslan, A. and Orcan, Y. 2002. Elastic–plastic Deformation of a Rotating Solid Disk of Exponentially Varying Thickness. *Mechanics of Material*. 34(7): 423-432.
- [4] Eraslan, A. N. and Argeso, H. Limit Angular Velocities of Variable Thickness Rotating Disks. 2002. *International Journal of Solids and Structures*. 39(12): 3109-3130.
- [5] Seireg, A. and Surana, K. S. 1992. Optimum Design of Rotating Disks. *ASME*. 92: 1- 10.
- [6] Ray, G.S., Sinha, B.K. 1992. Profile Optimization of Variable Thickness Rotating Disc. *Computers and Structures*. 42(5): 809-813.
- [7] Chern, J. M. and Prager, W. 1970. Optimum Design of Rotating Disks for Given Radial Displacement of Edge, *Journal of Optimization Theory and Applications*. 6: 161-170.
- [8] Fox, R. L. 1970. *Optimization Method for Engineering*. Addison - Wesley, London.
- [9] Cheu, T. C. 1990. Procedures for Shape Optimization of Gas Turbine Disks. *Computers & Structures*. 34(1): 1-4.
- [10] Luchi, M. L. Poggiali, A. and Persiani, F. 1980. An Interactive Optimization Procedure Applied to the Design of Gas Turbine Discs. *Computers & Structures*. 11(6): 629-637.
- [11] Farshi, B., Jahed, H. and Mehrabian, A. 2004. Optimum Design of Inhomogeneous Non-Uniform Rotating Discs. *Computers and Structures*. 82(9-10): 773-779.
- [12] Jahed, H., Farshi, B. and Bidabadi, J. 2005. Minimum Weight Design of Inhomogeneous Rotating Discs. 2005. *International Journal of Pressure Vessels and Piping*. 82: 35-41.
- [13] Brujic, D., Ristic, M., Mattone, M., Maggiore, P. and De Poli, G. P. 2010. CAD Based Shape Optimization for Gas Turbine Component Design. *Structural and Multidisciplinary Optimization*. 41(4): 647-659.
- [14] S. Derakhshan, S. N. Kasaeian. Design and Optimization of Axial Turbine for Small Hydropower, *Journal of Mechanical Engineerin (University of Tabriz)*, 43(2), pp. 31-40, 2013.
- [15] Gutzwiller, D. P. and Turner, M. G. 2010. Rapid Low Fidelity Turbomachinery Disk Optimization. *Advances in Engineering Software*. 41: 779–791.
- [16] Gunston, B. 2009. *The Cambridge Aerospace Dictionary*, 2nd ed. Cambridge University Press.
- [17] Meisl, C. J. 1988. Life-Cycle-Cost Considerations for Launch Vehicle Liquid Propellant Rocket Engine. *Journal of Propulsion and Power*. 4(2): 26-118.
- [18] Zhan, H., Zhao, W. and Wang, H. 2000. Manufacturing Turbine Blisks. *Aircraft Engineering and Aerospace Technology*. 72(3): 247-251.
- [19] Feiner, D. M. and Griffin, J. H. 2004. Mistuning Identification of Bladed Disks Using a Fundamental Mistuning Model-Part II: Application, *Journal of Turbomachinery*. ASME 126(1): 159-165.
- [20] Kostyuk, A. and Forlov, V. 1988. *Steam and Gas Turbines*, Translated from the Russian by V. Afanasyev, Mir Publishers Moscow.
- [21] Rosyid, A., Es-Saheb, M. and Yahia, J. H. 2014. Stress Analysis of Nonhomogeneous Rotating Disc with Arbitrarily Variable Thickness Using Finite Element Method. *Journal of Applied Sciences, Engineering and Technology*. 15: 3114-3125.
- [22] Zharfi, H. and Ekhteraei Toussi H. 2016. Effect of Temperature and Particle Distribution on Creep Behavior of FGM Rotating Discs (In Persian). *Journal of Mechanical Engineering*. 75(2): 51-59.
- [23] EN 1993-1-2: Eurocode 3: Design of Steel Structures - Part 1-2: General Rules - Structural Fire

Design.

- [24] Stump, F. V. Silva, E. C. N. and Paulino, G. H. 2007. Optimization of Material Distribution in Functionally Graded Structures with Stress Constraints. *Communications in Numerical Methods in Engineering*. 23(6): 535–551.